The dynamics of spawning acts by a semelparous fish and its associated energetic expenses

Cédric TENTELIER[1], Colin BOUCHARD[1], Anaïs BERNARDIN[1], Amandine TAUZIN[1], Jean-Christophe AYMES[1], Jacques RIVES[1]

[1]ECOBIOP, INRA, Univ. Pau & Pays Adour, 64 310 Saint-Pée-sur-Nivelle, France

Corresponding author: Cédric TENTELIER,
Univ. Pau & Pays Adour
Collège STEE – Campus de la côte basque
1 allée du parc Montaury
64 600 Anglet, France.
cedric.tentelier@univ-pau.fr

Abstract

1. During the reproductive season, animals have to manage both their energetic and gametic budgets. In particular, for semelparous capital breeders with determinate fecundity and no parental care, the depletion of energetic stock must match the depletion of gametic stock, so that individuals get exhausted just after their last egg is laid. Although these budgets are managed continuously, monitoring the dynamics of mating acts and energy expenditure at a fine temporal scale in the wild is challenging.

2. The goal of this study was to quantify the individual dynamics of spawning acts and the concomitant energy expenditure of female Allis shad (*Alosa alosa*) throughout the mating season in a short river.

3. Tri-axial acceleration, temperature and pressure data collected by eight individual-borne accelerometers for one month were analysed to i) detect the timing of spawning acts, ii) estimate energy expenditure from tail beat frequency and water temperature, and iii) monitor changes in body roundness.

4. Female shad performed on average 15.75 spawning acts, in 4.87 short volleys of 3.23 acts separated by 3.55 resting nights. The timing of spawning acts was influenced by oocyte maturation, temperature and social factors. Shad were more active at night and in warmer water. According to an energetic model based on American shad (*Alosa sapidissima*), they consumed on average 0.19 $kJ.min^{-1}$ and 7193 kJ over one month of spawning activity, but parameters from American shad may not be adapted to Allis shad. They died on average four days after their last spawning act, having lost 42% of their weight, but all with residual oocytes. The acceleration-based indicator of body roundness was correlated to condition coefficient, and globally decreased through the spawning season, although the indicator was noisy and did not match changes in energy expenditure.

5. Despite significant individual variability, our results indicate that female shad exhausted their energetic stock faster than their egg stock. This mismatch might be accentuated by habitat fragmentation and water warming. Although perfectible, the three complimentary analyses of acceleration data are promising for *in situ* monitoring of energy expenditure related to specific behaviour.

Keywords

Accelerometer, biologging, clupeid, energy budget, reproductive effort, semelparity, temperature, thinning.

Introduction

The energy acquired by living organisms through nutrition is allocated to survival and reproduction, and natural selection is expected to favour optimal allocation, resulting in life-histories that maximize Darwinian fitness in the environment where evolution occurs (Pianka, 1976; Roff, 1993; Stearns, 1992). When adult survival is low compared to juvenile survival, extreme reproductive effort (in gametogenesis, mating behaviour and parental care) can be selected and semelparity may arise, in which individuals die after their first and only breeding season. Semelparity is often accompanied with capital breeding, so that reproduction relies on energy reserves constituted before the breeding season (Bonnet, Bradshaw, & Shine, 1998). Although semelparity has been quoted as "big bang reproduction", its broad definition encompasses cases where individuals breed in several bouts within a breeding season (Hughes, 2017). For example, Pacific salmons of the genus *Oncorhynchus* are paragons of semelparous capital breeders but dig several nests in which they spawn with several mates. Likewise, many insect species do not feed during their very short adult life and qualify as semelparous despite laying several clutches of eggs within a few days. Furthermore, in species with no parental care, the optimal allocation should result in individuals dying just after their last progeny is produced, and deviation from optimality consists in individuals either surviving after their last egg is laid, or dying of exhaustion while still bearing unlaid eggs (Heimpel & Rosenheim, 1998). Hence, the schedule of breeding events and the dynamics of energy expenditure during the breeding season, which may be steep in semelparous capital breeders, is a crucial aspect of reproductive strategy. Anthropic perturbation of this energy dynamics, through change in temperature, habitat fragmentation or pollution, is crucial to the conservation of many populations.

Tracking the schedule of breeding events and the dynamics of energy expenditure of breeding individuals in the wild is technically challenging. The timing of breeding events along the breeding season requires thorough observation of repeatedly detectable individuals, for example through video supervision of highly sedentary individuals (e.g. Borgia, 1985). Energy expenditure has been monitored

at the population level, by quantifying energy reserves on different individuals sampled at different stages of the breeding season (e.g. Andrew P Hendry & Berg, 1999). In some cases, the same individuals were captured at the beginning and at the end of the breeding season, and the energy expenditure quantified with difference in weight (Anderson & Fedak, 1985; Rands, Houston, & Cuthill, 2006), body composition (Casas et al., 2005; A. P. Hendry & Beall, 2004), or concentration of plasma metabolites (Gauthey et al., 2015). Likewise, the turnover of ^{18}O and ^{2}H from doubly labelled water quantifies the average field metabolic rate at the individual level between two sampling occasions (Nagy, Girard, & Brown, 1999). All these experiments give a good idea of the total energy expenditure over the whole breeding season but often lack the temporal resolution to document the longitudinal dynamics of energy expenditure all along the breeding season. When individuals are frequently observed during the breeding season, daily activity budgets associated to laboratory-measured activity-specific energetic costs can increase the temporal resolution of energy expenditure (Goldstein, 1988).

With the advent of bio-logging, the temporal resolution of individual data collected in the field has tremendously increased. Electromyograms, heart rate data loggers and accelerometers put on animals released in the wild can continuously sample at high frequency data that are relevant to activity. When calibrated in laboratory experiment, these data can even be converted to energy expenditure, in Joules or O_2 consumption rate (Collins et al., 2016; Groscolas, Viera, Guerin, Handrich, & Côté, 2010; Hicks et al., 2017; Wilson et al., 2006). These loggers are often coupled to other animal-borne loggers which measure environmental variables such as temperature, light or pressure, thereby allowing to refine the estimation of energy consumption or to test ecophysiological predictions (Handrich et al., 1997; Wright, Metcalfe, Hetherington, & Wilson, 2014). Among these loggers, accelerometers have been increasingly used, and advances in their energetic efficiency now allows to record high-frequency data for weeks or months, making them valuable tools for longitudinal studies of breeding behaviour in many organisms. In this context, acceleration data can quantify both the overall movement of tagged individuals, and the number and temporal distribution of key behaviours, such as mating events, provided they produce a typical acceleration pattern (Brown, Kays, Wikelski, Wilson, & Klimley, 2013).

Allis shad (*Alosa alosa* L.) is an anadromous clupeid fish distributed along Atlantic coast of Europe, from Portugal to the British Isles, with the main populations dwelling in the Garonne, Dordogne and Loire rivers, France (Baglinière & Elie, 2000). Most of these populations have plummeted since the beginning of the 21st century, with no clear unique cause but suspicion of overfishing, predator introduction, or the degradation of freshwater and marine environment (Rougier et al., 2012). Across its distribution, Allis shad is considered a semelparous species, although spawning marks on scales suggest that a very small proportion of individuals may spawn on two consecutive years (Mennesson-Boisneau & Boisneau, 1990; Taverny, 1991). After having spent a few months in freshwater and four to six years at sea, shad undertake upstream migration during which they fast, thus qualifying as capital breeders. Migration is accompanied by gonad maturation, with females bearing between 13 000 and 576 000 eggs and reaching an average gonad somatic weight ratio of 15% on spawning grounds (Cassou-Leins & Cassou-Leins, 1981; Taverny, 1991). Spawning typically occurs at night in a 0.3 to 3 meter-deep glide, and the spawning act consists in at least one male and one female swimming side by side during five to ten seconds in three to five circles of one meter in diameter, and thrashing the water surface with their tail (Baglinière & Elie, 2000). The typical splashing noise (35 dB at one meter) can be heard and recorded from the river bank, and the number of splashes recorded during the spawning season is often used as an indicator of the number of spawners in a population (Chanseau, Castelnaud, Carry, Martin-Vandembulcke, & Belaud, 2004). Although very few data are available, the number of splashes recorded upstream from dams where migrating shad were counted suggest that females perform on average five to twelve spawning acts during the season (M. Acolas et al., 2006; Fatin & Dartiguelongue, 1996). The temporal distribution of splashes within a night follows a Gaussian distribution centred on 2 AM and spanning from 10 PM to 6 AM (Cassou-Leins & Cassou-Leins, 1981). The spawning season spans from early-May to late July, and the spawning activity increases with increasing water temperature and decreasing flow (Baglinière & Elie, 2000). Although the temporality of reproduction is well documented for some thoroughly monitored populations, no data exist at the individual level. Likewise, although samples of different individuals at different times during the migration have shown

dramatic changes in somatic mass and tissue composition (Bengen, 1992; Cassou-Leins & Cassou-Leins, 1981), no longitudinal data exist at the individual level during the spawning season.

This study aimed at describing the activity and change in body condition of Allis shad females throughout the breeding season. Three main aspects were investigated using accelerometers: 1) global activity was quantified as tail beat frequency and vector of the dynamic body acceleration, 2) spawning events were detected thanks to characteristic acceleration pattern, and 3) body roundness was assessed by the angle between the accelerometer attached to the fish and the vertical. The temporal evolution of these variables was related to each other and to other individual variables such as individual size and weight of eggs remaining at death, and to environmental parameters such as water temperature.

Methods

Study system

This study was conducted in spring 2017 and 2018 in the Nivelle, a 39 km long coastal river situated in the Northern Basque Country, France, and draining a 238 km² basin. The downstream limit of the study zone was the impassable Uxondoa weir, situated 12 km upstream from the river mouth (43°21'40.64"N, 1°35'13.99"W), and equipped with a vertical slot fishway and a trap where a yearly average of 230 (min = 26; max = 688) migrating shad have been counted since 1996, with less than 30 individuals per year since 2015. Five kilometres upstream from Uxondoa stays another impassable weir equipped with a fishway and a trap, where shad are almost never captured.

Tagging procedure

The Uxondoa fish trap was controlled daily throughout spring. Nine female shad were captured and tagged in 2017 and 15 in 2018. The tagging procedure was quite similar to Breine (2017) for twaite shad (*Alosa fallax*). Each individual was anesthetized in a bath of 15 mg/L benzocaine diluted in river water. It was weighed, its fork length was measured, and it was tagged with a radio transmitter

emitting at a unique frequency (F2020, ATS, Isanti, MN, USA) and a three-dimensional accelerometer (WACU, Atesys-Montoux, Huguenau, France). For tagging, each fish was kept in a 20 L tank filled with anaesthetic solution. A water pump placed in the fish's mouth and a stone bubbler ensured a good circulation of aerated water during the tagging procedure. Adjustable plastic plates covered with foam were placed vertically against both flanks to maintain the fish in an upright position, with only its back being above water surface. The radio transmitter and the accelerometer were cleaned with a povidone iodine solution (Betadine®) and dried with surgical cotton. The two Teflon-coated metallic wires of the radio transmitter were inserted approximately 1 cm under the dorsal fin through sterile hollow needles. The hollow needles were then removed, and the metallic wires were passed through holes drilled in the accelerometer's lug, secured with plastic eyelets and aluminium sleeves, and the extra length was cut. The radio transmitter and the accelerometer weighed 8.6 g and 9 g, respectively, so the weight was balanced on both sides of the fish. After tagging, each fish was placed in a 50 L box filled with river water, and released upstream from the weir upon waking. This tagging procedure was approved by the ethical committee of the French region Nouvelle Aquitaine for birds and fishes (authorization #2016020116037869).

Tracking and recapture

From its release at Uxondoa weir until its death at the end of the spawning season, each tagged shad was localized daily using a mobile receiver (R2100, ATS, Isanti, MN, USA) and a loop antenna, in order to check whether it was still alive and in the study area. The radio transmitters were set to double their pulsing rate after 8 h of total immobility. Within two days after double pulse was detected, the dead fish and the tags were recovered by snorkelling. The whole fish and its ovaries were immediately weighed to compute the final condition coefficient and the final ovary index, computed as the ratio of ovary weight (in grams) on the cube of body length (in centimetres).

Analysis of acceleration data

The accelerometer model used in this study recorded acceleration between -8 g and +8 g (1 g = 9.81 m.s^{-2}) in each of the three dimensions at an average frequency of 50 logs per second. Every second, it also recorded, temperature, pressure, date, time and the exact number of acceleration logs within the past second. Logging data for one month resulted in a 3.3 Gb text file containing 129.6 million rows. Acceleration data can be split in two components which provide two types of information on animal behaviour. The static component of acceleration, obtained by applying a low-pass filter to raw data (typically averaging raw data across a few seconds), corresponds to the acceleration due to gravity. For a given altitude and latitude, this acceleration is constant (~9.81 m.s^{-2}) but its distribution across the three axes of the accelerometer informs on the orientation of the accelerometer compared to perfect verticality, which is usually interpreted in terms of animal posture (upright, lying down on either side…). The dynamic component of acceleration, obtained by applying a high-pass filter (typically removing the static component from raw data), informs on the movement of the animal. This can be used quantitatively, to assess overall activity, or qualitatively, to detect specific behaviour associated to peculiar acceleration patterns. In this study, both components were used to address three types of questions, as described below.

The static, gravitational, component on each axis *i* (*x, y* or *z*) was extracted from the raw signal at each time *t* by replacing each data point $\overrightarrow{A_{\iota,t}}$ by the average of the points within a window of width *w* centred on *t*, so that $\overrightarrow{SA_{\iota,t}} = \frac{1}{w}\sum_{j=t-w/2}^{j=t+w/2}\overrightarrow{A_{\iota,J}}$. Contrary to what is usually done, these data were not used to assess the posture of the fish, as no known behaviour in shad involves change of posture. Instead, we hypothesized that it may reflect the shape of the fish. Indeed, since the accelerometer was pinned on the dorsal part of the fish's flank, the angle θ between the *x*-axis of the tag and the vertical may be linked to the roundness of the fish, a proxy of its energetic reserves. This angle could be computed at any data point of static acceleration, as $\theta_t = cos^{-1}(\overrightarrow{SA_{x,t}})$, where θ_t is the angle at time *t* and $\overrightarrow{SA_{x,t}}$ is the static acceleration computed on the *x*-axis at time *t* (Fig. 1). To track change in body roundness

through the season, θ was estimated for each fish from $\overrightarrow{SA_{x,t}}$ computed over *w*=180 000 points (*i.e.* 1 h at a 50Hz sampling frequency) every eight hours (6AM, 2PM, 10PM), from its release until its death.

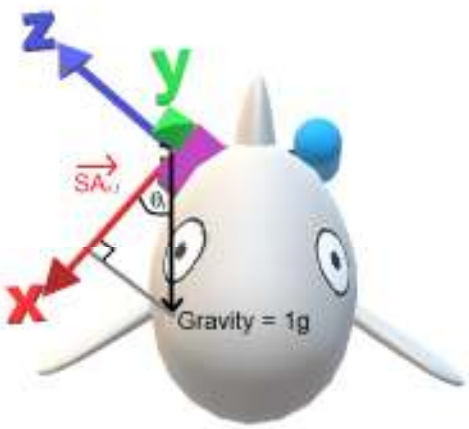

Figure 1. Allis shad were tagged with a radio transmitter on the left flank and an accelerometer on the right flank. The accelerometer continuously recorded acceleration on three axes. The static component of acceleration recorded on the x-axis at time *t*, $\overrightarrow{SA_{x,t}}$, corresponds to the orthogonal projection of gravity, which is vertical by definition, on this axis. Hence, the angle θ between the x-axis and the vertical can be computed for any time *t* as $\theta_t = cos^{-1}(\overrightarrow{SA_{x,t}})$

The dynamic component of acceleration was computed at every time point on each dimension *i* ($\overrightarrow{DA_{i,t}}$) as the raw signal minus the static acceleration. This was used to quantify the activity of the fish Tail Beat Frequency (TBF), computed as the number of zero-crossings of $\overrightarrow{RDA_{z,t}}$ per second, which is well correlated to swim speed and dioxygen consumption in shad (Leonard, Norieka, Kynard, & McCormick, 1999). TBF can be computed at every instant, but for further analysis we used average computed for every minute. Along with the temperature recorded by the individual logger, this was used to estimate energy consumption for every minute of the individual spawning season, using equations established by Leonard et al. (1999) and Castro-Santos & Letcher (2010) on American shad, *Alosa sapidissima*. TBF (beats.s^{-1}) was first converted to swim speed (U, in body length.s^{-1}), as:

$$U = (TBF \times 60 - 32.9) / 86 \quad \text{(Equation 1)}$$

Then, oxygen demand (MO_2, in mmol $O_2.kg^{-1}.min^{-1}$) was computed as the following function of swim speed and temperature (T, in °C):

$$MO_2 = 60 \times 10^{(0.084 + 0.0363 \times T + 0.267 \times U)} \quad \text{(Equation 2)}$$

Then, MO_2 was converted to the rate of energy consumed per kg of fish (E_m, in $kJ.kg^{-1}.min^{-1}$), assuming that 0.4352 kJ of somatic energy are burnt per mmol O_2 (Brett & Groves, 1979). To express the energy consumed by each fish for each minute, E_m must be multiplied by fish mass (M, in kg). However, since energy consumption continually reduces fish mass, we iteratively modelled fish mass and energy expenditure at each minute of the spawning season. For this, we assumed that shad get 69% of their energy from lipids and 31% from proteins to fuel their metabolism (Leonard & McCormick, 1999), and that one gram of fat yielded 39.54 kJ against 23.64 kJ per gram of protein (Craig, Kenley, & Talling, 1978) , so the energy consumed (E_t, in kJ) and fish mass (M_t, in kg) at the tth minute were:

$$E_t = MO_2 \times 0.4352 \times M_t \quad \text{(Equation 3)}$$

$$M_t = M_{t-1} - 0.001 \times E_{t-1} / (0.69 \times 39.54 + 0.31 \times 23.64) \quad \text{(Equation 4)}$$

The dynamic acceleration was also used to count the number of spawning events performed by each tagged shad. To do this, the acceleration pattern typical of spawning act was first described in a controlled experiment and then searched in the field-collected data. To characterize the typical pattern associated with spawning act, a male and a female shad were captured at Uxondoa trap, tagged as described above, and observed for one month (June 2016) in a basin (400 m², 0.6 m water depth) at the INRA experimental facilities in St Pée/Nivelle. Eight spawning acts were recorded on video or audio recordings of spawning acts were obtained, which could be paralleled with acceleration data. The typical pattern of acceleration associated to the spawning act was a rise in the norm of the 3D acceleration vector, which stayed above 3g for at least 3 seconds, mainly driven by acceleration on the z-axis corresponding to TBF reaching up to 15 beats per second. A decrease of hydrostatic pressure

240 was typically associated to this pattern, due to the fish reaching the water surface during the spawning
241 act. These criteria for identification of spawning acts were robust, as they were always detected when
242 spawning was visually observed (no false negative) and never observed when spawning was not
243 visually observed (no false positive). These criteria were implemented in an algorithm to scan the
244 accelerograms collected in the field in 2017. This automated identification was validated by visual
245 comparison of accelerogram sequences automatically identified in 2017 with sequences of
246 acknowledged spawning acts recorded in 2016.

247 Finally, the exact timing of each individual's death was detected as a clear change in the acceleration
248 signal, where the gravitational component indicated that the fish switched from upright posture to
249 lying on its side or upside down, and the only dynamic component left was the tenuous jiggling due to
250 water flowing over the tag.

251 Statistical analysis

252 Separate Spearman correlations were used to test the link between the number of spawning acts
253 performed by each individual and its body length, date of arrival in the study zone, initial weight and
254 condition coefficient, final ovary index, weight and condition coefficient, and weight loss. Although the
255 small number of data did not allow to perform multiple regression, Bonferroni correction was applied
256 to limit the inflation of alpha error. A zero-inflated mixed regression (using glmmTMB package on R
257 software Brooks et al., 2017; R Development Core Team, 2008) was used to test the effect of
258 temperature on the number of spawning acts performed by each individual on each night. The
259 Binomial component of the model informed on the effect of temperature on the probability to perform
260 any spawning act, while the Poisson component tested the effect of temperature on the number of
261 spawning acts performed. Individual was used as a random effect on both components. At a finer time
262 scale, we tested whether females spawning in the same night synchronized their spawning acts. To do
263 this, we performed 10 000 permutations of the hour of spawning acts recorded along all nights, and
264 compared the median of the delay to the nearest spawning act for actual data and for simulated data.

Because our aim was not to test the synchrony between acts performed by the same female, only the first act performed by each female on a given night was considered in this analysis.

As mentioned above, TBF was computed for every minute of each individual's spawning season, to track its energy expenditure. As an indicator of fish activity, average TBF was also aggregated over eight-hour time windows corresponding to three periods of the day: morning (6AM-2PM), afternoon (14PM-10PM) and night (10PM-6AM). The effect of the period of day, temperature, the occurrence of spawning acts and the recency of tagging on TBF were tested with a linear mixed model with individual random intercept. Based on visual observations on spawning grounds, shad were expected to be more active at night than in the morning and the afternoon, to be more active near spawning acts, and to increase their activity with water temperature. To test whether capture, anaesthesia and tagging reduced shad activity, recency of tagging was included in the linear mixed model as an indicator of whether the fish was released for less or more than 72 hours. Moreover the temperature to which shad were exposed is expected to change with the period of the day and with depth, with warmer water in the afternoon and at shallow depth. We tested this with a linear mixed model using temperature as the response variable, individual random intercept, and period and pressure as fixed effects. Visual observations on spawning grounds also suggest that shad dwell deep in pools during the day and are active near the surface of spawning grounds during the night. This was tested with a linear mixed model using pressure as the response variable, period as the fixed effect and individual random intercept.

We tested three predictions resulting from the hypothesis that the angle θ between the x-axis of an individual's accelerometer and the vertical was an indicator of body roundness. First, the expected positive association between Fulton condition coefficient (100*weight (in grams)/length (in centimetres)^3) and θ was tested with a linear mixed model with individual random intercept, since each individual was weighed at release and after death, so two values were obtained by individual. Second, a linear mixed model, with individual random intercept and slope was used to test whether θ

decreased over time since individual release. Third, to test if change in θ over the breeding season was proportional to change in condition, a linear regression was fitted between the differences in θ and in Fulton condition coefficient from release to death. Finally, to test whether the decrease in θ could be linked to temperature and activity and spawning acts, we fitted a linear mixed model with individual random intercept, period of the day, temperature, TBF and occurrence of spawning acts during the period as fixed effects, and the difference in θ computed for the period and the next one as the dependent variable. All mixed models were fitted using the package lme4 for R (Bates, Maechler, Bolker, & Walker, 2014), and significance of fixed effects was tested using the likelihood ratio test (LRT) between the model including the effect and the nested model excluding it.

Results

The nine female shad tagged in 2017 survived between 20 and 37 days (mean=26 days), and all tags were retrieved within one or two days after fish died, although one tag stopped recording data after ten days. The 2018 campaign was much less successful: two fish died one week after tagging, before any spawning acts were recorded; two fish lost their tags three and four days after tagging. The eleven remaining fish were radio tracked throughout the spawning season, until two exceptional floods (on June 7th and 16th) flushed them down to the estuary where the high water conductivity prevented further radio tracking, and therefore tag retrieval. Hence, among the 25 tagged shad, only eight fully exploitable and one partially exploitable accelerograms could be collected.

Table 1. Biometry of the nine Allis shad females tagged with accelerometers and retrieved dead after the 2017 spawning season in the river Nivelle. The accelerometer borne by individual 9 stopped logging on the 9th of June.

Individual	Date of capture	Initial weight (g)	Initial total	Date of death	Final total weight (g)	Final weight of ovaries (g)

			length (cm)			
1	05/16	1450	530	06/22	676	45
2	05/23	1810	575	06/19	1131	128
3	05/24	1635	585	06/19	924	26
4	05/26	1700	585	06/17	1021	110
5	05/26	1565	583	06/16	1044	50
6	05/27	1320	560	06/21	701	42
7	05/27	1635	570	06/25	914	96
8	05/27	1410	570	06/16	827	79
9	05/29	1720	590	06/17	1130	141

According to their accelerograms, the eight female shad performed 7, 9, 12, 14, 14, 17, 24 and 26 spawning acts (mean=15.75). The total number of spawning acts performed by each female was correlated to none of the individual variables tested (Spearman's correlation for body length: S=132.36, P=0.135; date of arrival in the study zone: S=78.295, P=0.873; initial weight: S=134.6, P=0.114; date of death: S=70.337, P=0.7; final weight: S=132.29, P=0.136; final ovary index: S=80.982, P=0.933; weight loss: S=97.157, P=0.711). For each female, spawning acts were distributed in three to six nights (mean=4.87) each separated by zero to eight nights (mean=3.55) without spawning acts, resulting in individual spawning seasons ranging from 14 to 24 nights (mean=18.12) from the first spawning act to the last (Fig. 2). The tagged females performed their first spawning act zero to eight days after tagging (mean=3). Only on eight occasions did a female perform a single spawning act during a night, so the 137 remaining acts were performed in volleys. At the individual level, these volleys contained from two to eight acts (mean=3.23) and lasted from two to 84 minutes (mean=29.7). The mixed zero-inflated Poisson regression indicated that water temperature during the night had a positive effect on the probability that a female performed at least one spawning act (negative effect

on the zero inflation; z=-1.95, P=0.05) but no effect on the number of spawning acts in the volley (the Poisson component; z=-1.44, P=0.15). Cumulated over all the season, the temporal distribution of spawning acts within the night followed a Normal distribution, centred on 3AM, with 95% of spawning acts occurring between 0:30AM and 5:30AM. However, the permutation test on the hour of spawning acts indicated synchrony between acts performed by different females on the same night: the median of the time lag to the nearest act was one hour for observed data, which corresponds to the first percentile of simulated data (Fig. 3). The shad died 44 to 182 hours (mean=98.62) after their last spawning act. They had lost between 33% and 53% of their weight (mean=42%), and their ovaries weighed 25.9 to 141.5 g (mean=79.7). No correlation was found between the two variables (Pearson's S=102; P=0.619).

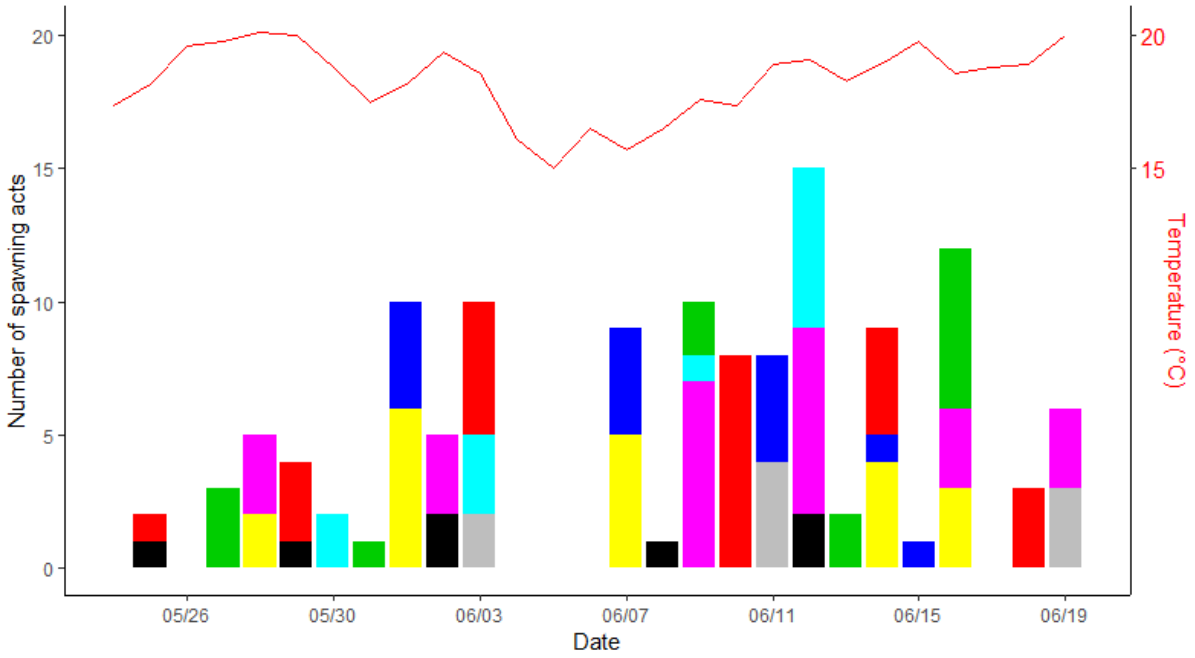

Figure 2. The temporal distribution of spawning acts by eight Allis shad females in the river Nivelle in spring 2017. Black, red, green, navy blue, light blue, pink, yellow and grey correspond to individuals #1 to #8 in Table 1. The line represents the average water temperature measured each night between 10PM and 7AM.

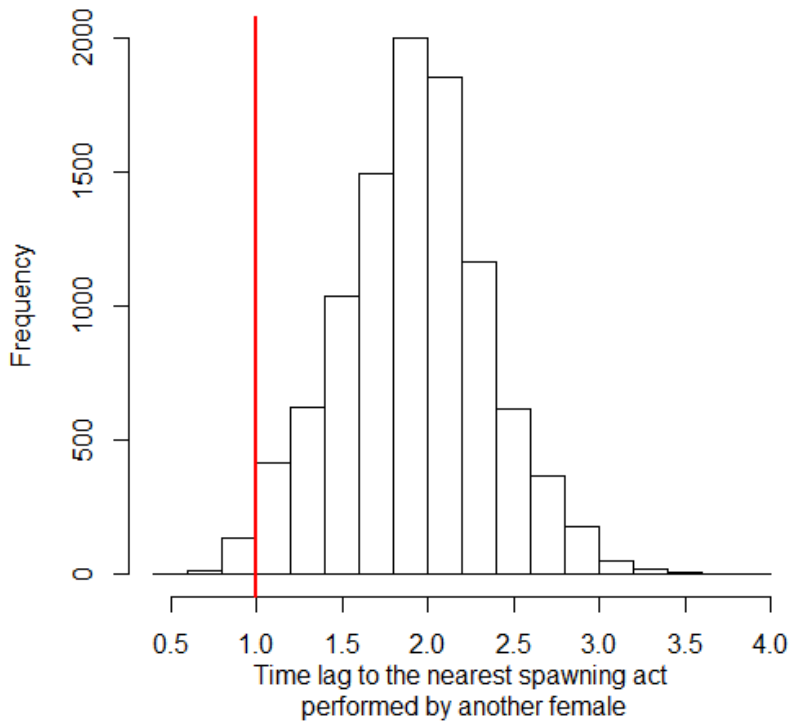

Figure 3. Synchrony of Allis shad spawning acts within a night. The red vertical line represents the median of the time lag between nearest spawning acts for observed data. The histogram represents the same thing for 10 000 permutation of the hour of the acts. The observed value corresponds to the first percentile of the simulated values.

Average tail beat frequency (TBF), temperature and pressure were computed for 312 840 minutes across all individuals' spawning seasons (eight complete and one partial). Average TBF ranged from 1.3 to 9.5 beats per second (mean=3.2), temperature ranged from 13.5 to 23.8°C (mean=18.3), and pressure ranged from 1 012 to 1 400 hPa (mean=1 191). From these data and equations 1 to 4, the estimated instantaneous rate of energy expenditure ranged from 0.06 to 3.14 $kJ.min^{-1}$ (mean=0.19), and energy expenditure cumulated by each individual from initial capture to death ranged from 4856 to 9743 kJ (mean=7193) (Fig. 4). The corresponding weight loss was estimated to range from 140 to 278 g (mean=205), making from 10% to 19% of initial weight (mean=13%). The predicted and observed proportions of weight lost during the season tended to be positively correlated, although this was not significant (Spearman S=26; P=0.06).

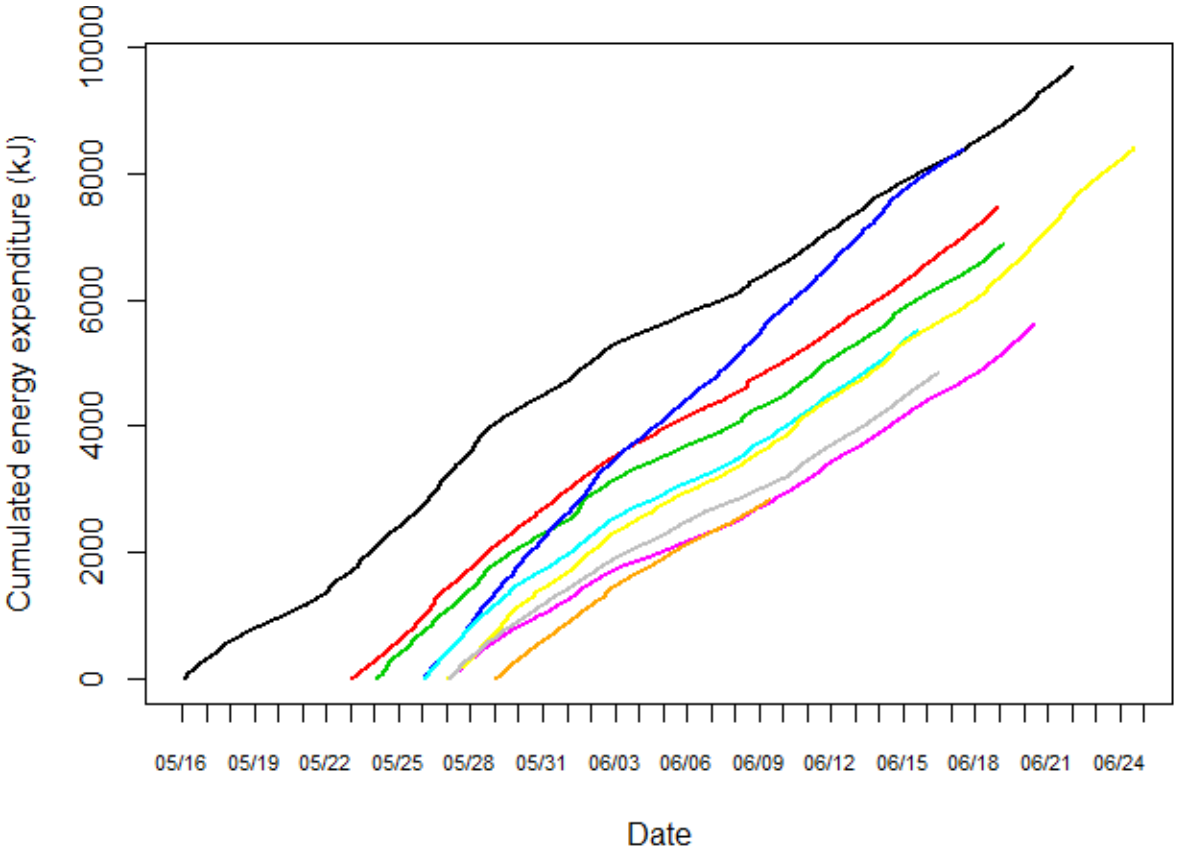

Figure 4. Dynamics of energy expenditure by nine Allis shad females throughout the spawning season. Energy expenditure was computed for every minute from data on tail beat frequency, water temperature and initial fish weight, using Equations 1 to 4. Each colour represents an individual, with the same correspondence as in Fig. 3, and the additional orange line corresponds to individual #9, the accelerometer of which stopped logging on the 9th of June.

Aggregating TBF, temperature and pressure data over eight-hour periods (morning: 6AM-2PM, afternoon: 14PM-10PM, night: 10PM-6AM) produced 649 periods. Shad underwent lower pressure during the night (mean=1.166 hPa) than during the morning and afternoon (mean=1.204 hPa for both periods; t=14.3; LRT=226.9; p<0.0001), corresponding to a depth difference of 38 cm. Water temperature to which shad were exposed depended on both the period of the day and pressure (LRT=42.777; p<0.0001). Although raw data suggest that water was warmer in the afternoon than in

the night, which was warmer than in the morning, it also refreshed with increasing pressure (t=-5.286; LRT=26.12; p<0.0001), and shad were exposed to lower pressure in the night, as indicated above. Hence the linear mixed model including the effect of both pressure and period indicate that the effect of period was such that shad encountered the freshest water in the night, warmer in the morning (t=0.117) and the warmest in the afternoon (t=3.857). The linear mixed model fitted on TBF indicated a significant positive effect of temperature (LRT=111.56; p<0.0001; t=11.039), and a significant effect of the period of day (LRT=22.387; p<0.0001): TBF was higher during night time (10PM-6AM) than during the afternoon (2PM-10PM; t=-3.37) and the morning (6AM-2PM; t=-4.648). Moreover, TBF was higher in the three days following tagging and release than during the rest of the survey (LRT=20.78; p<0.0001; t=4.597), and was higher in the periods when the female performed spawning acts (LRT=53.86; p<0.0001; t=7.496).

The initial and final θ angle between the x-axis of the accelerometer and the vertical was positively related to the individual's Fulton coefficient of condition (t=4.11; LRT=10.82; P=0.001 Fig. 5.a). Moreover, the θ angle decreased over time for all individuals (t=-4.31; LRT=10.07; P=0.001, Fig. 5.b), with a slope of -0.24 degree per eight hours. However, the difference of the θ angle between initial capture and death was not related to weight loss between initial capture and final recapture (slope of the linear regression=-0.046; t=-0.899; P=0.403). The difference in the value of the θ angle between the beginning and the end of a period was not affected by TBF (LRT=0.337; P=0.5616; t=-0.581), temperature (LRT=0.235; P=0.6282; t=0.484) or occurrence of spawning acts (LRT=0.491; P=0.4834; t=0.701). However a significant effect of the period of the day was found (LRT=48.869; p<0.0001), with θ decreasing more during the night than during the morning (t=-7.123) or the afternoon (t=-3.673).

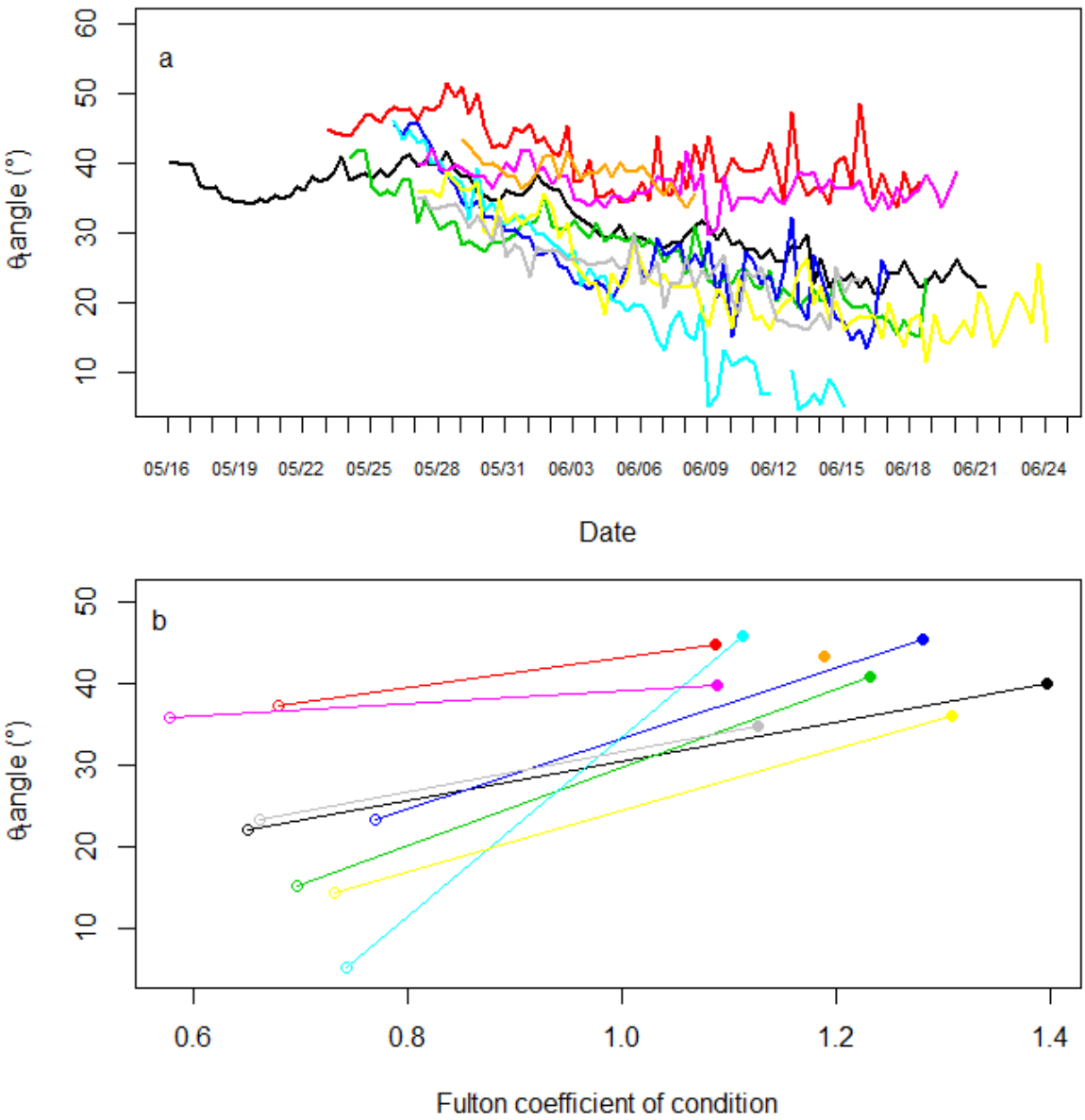

Figure 5. The θ_t angle between the x-axis of the accelerometer and the vertical as an indicator of fish thinning. a) Temporal evolution of θ computed each day along the spawning season for nine Allis shad b) Relationship between Fulton coefficient of condition and θ_t angle at initial release (filled symbols) and at recapture after death (open symbols). Each individual is represented with the same colour as in Figs. 3 and 4.

Discussion

In this study, we used acceleration data to quantify the dynamics of spawning acts, energy expenditure and body roundness of Allis shad females throughout their spawning season. The results indicate that the spawning schedule of shad females, although constrained by the serial maturation of oocyte batches, is also influenced by temperature and social factors. Tail beat frequency and water temperature recorded by the loggers allowed to estimate the energy expenditure from equations obtained on American shad, but differences between these two species may have biased our estimate. Finally, the original use of gravitational acceleration to monitor fish thinning, although perfectible seems a promising method in animal ecology.

Collecting significant individual acceleration data for several weeks in the wild can be challenging, and our data on shad, although concerning only eight individuals, can be considered a methodological success. Allis shad is considered a very fragile fish, hardly enduring manipulation, with high mortality rate or long downstream movement following gastric implantation of acoustic or radio tags (Steinbach, Gueneau, Autuoro, & Broussard, 1986; Tétard et al., 2016). In this context, the good survival, and seemingly normal behaviour of the individuals tagged in this study is noteworthy. Of the 22 fish that did not lose their tags, only two died after one week, but the other 20 survived for several weeks. Although the dead individuals retrieved showed clear depigmentation and a slight erosion of the tegument under both radio tag and accelerometer, neither severe abrasion nor fungal proliferation was observed, even after one month in water a 18° C. Eleven individuals moved several kilometres downstream, but only after the exceptional floods of 2018, which have probably also wiped away untagged shad, especially after the spawning season. Regarding this, although the small size of the river maximised our chances to retrieve dead fish and their tags, it also increased the risk that the fish were wiped to the sea, where radio signals could not be detected anymore. Although the summed weight of the accelerometer and the radio tag represented only 1% of the fish's initial weight, the externally attached tags have increased the drag, which could have disturbed swimming and spawning

426 behaviours. However, the eight females for which complete accelerograms were retrieved all
427 spawned, and the median of 14 spawning acts was slightly above the five to twelve acts per individuals
428 estimated by Acolas *et al.* (2006) and Fatin & Dartiguelongue (1996). Moreover, three individuals
429 spawned as soon as the first night following tagging, so tagging did not impair spawning. Tagging did
430 not seem to impair swimming activity either, as tail beat frequency (TBF) was not lower in the three
431 days following tagging than in the remaining of the season. TBF was actually higher during the first
432 three days, probably because the fish were finishing their upstream migration, before settling near
433 spawning grounds (unpublished radio tracking data). This absence of negative impact suggests that
434 external tagging, provided fish are continually kept immerged and rapidly handled, is a suitable tagging
435 technique for Allis shad (see also Breine et al., 2017 for Twaite shad; and Jepsen, Thorstad, Havn, &
436 Lucas, 2015 for other fishes). For accelerometers and environmental sensors, external attachment is
437 often the only option anyway, but tag placement on the fish is crucial to collect reliable data with the
438 least individual effect. Is this study, accelerometers were attached under the dorsal fin, which did not
439 impair swimming yet allowed to detect tail beats of shad, which use carangiform locomotion.

440 Some known aspects of shad spawning activity were confirmed and refined by our results, such
441 as the effect of temperature on activity and the number of spawning acts per individual. The analysis
442 performed at the individual level confirmed visual observations made on spawning grounds (Baglinière
443 & Elie, 2000), that shad were more active (higher TBF) and spent more time near the surface at night
444 than during the day, they spawned exclusively at night and were more active during the nights when
445 they spawned than when they did not. Shad were also more active and more likely to spawn when
446 temperature increased. But our individual-based monitoring also revealed features of shad spawning
447 behaviour that could not be documented by previous visual observations of undifferentiated
448 individuals. The average number of spawning acts per female was 15.75, and ranged from 7 to 26. So
449 far, the average individual number of spawning acts was indirectly estimated to be either five (Acolas
450 et al., 2006) or 12 (Fatin & Dartiguelongue, 1996) by counting the number of acts heard upstream a
451 dam where all passing individuals were counted. Such method provides no estimate of interindividual

452 variability. Also, in a first attempt to work at the individual level, Acolas et al. (2004) marked three
453 females and three males with acoustic tags, and based on the number of detections of the tags near
454 the surface (assessed by the reception power by hydrophones immersed at different depth), estimated
455 that zero, one and two acts were performed by the females and three, 38 and 60 acts by the males.
456 Here, despite a small sample, we estimated a more representative distribution of the number of acts
457 per individual, as their detection on accelerograms is certainly more reliable than the method used by
458 Acolas et al. (2004). This distribution will be crucial to build a model estimating the number of shad in
459 a river from the acoustic survey of spawning acts, as it is routinely done in French rivers (e.g. Chanseau
460 et al., 2004). The number of acts per female could be correlated to none of the few biometric variables
461 collected, but the very small sample implied a weak statistical power.

462 Acceleration data collected at the individual level throughout the spawning season also
463 allowed to precisely describe the spawning schedule of shad females. The individual spawning seasons
464 ranged from 14 to 24 nights between the first and the last spawning events, while the interval between
465 the first and last acts for all tagged females was 25 days. This indicates that each female was active for
466 most of the population's spawning season. The individual spawning season was punctuated by three
467 to six regularly spaced nights of activity, each generally corresponding to volleys of two to eight acts
468 performed in a few tens of minutes. The schedule of spawning acts must be constrained by the
469 fragmented maturation of oocytes (Cassou-Leins & Cassou-Leins, 1981), but also depended on
470 temperature. Interestingly, while data collected at the population level indicate that spawning activity
471 increases with temperature, our data collected at the individual level indicated that temperature
472 increased the probability that some acts were performed during the night, but not the number of acts
473 performed. In fact, two results suggest that the dynamics of spawning acts within a night may be
474 influenced by social factors. First, the temporal proximity of acts performed by a given female in a
475 given night, and the high proportion of acts performed without oocyte expulsion reported by Langkau
476 et al. (2016) remind of female trout's 'false orgasm' (Petersson & Jarvi, 2001) or female lamprey's
477 'sham mating' (Yamazaki & Koizumi, 2017). For both of these species, it has been suggested that

478 repeated spawning simulations enable the female to exert mate choice, by both exhausting the sperm
479 stock of an unwanted courtier and signalling its mating activity to peripheral males. Second, spawning
480 acts of different females in a given night were more synchronous than expected from the hour of
481 spawning acts across all nights of the season. This suggests that a female which is ready to spawn
482 (mature batch of oocytes) in a propitious night (warm temperature) may trigger its spawning acts when
483 another female does so. Such fine scale synchrony may again affect sexual selection, reducing the
484 environmental potential for polygyny by making it difficult for the same male to monopolize several
485 females at the same time (Emlen & Oring, 1977). The final point in the spawning schedule of
486 semelparous organisms is death, which struck female shad two to seven days after their last spawning
487 act, and before they laid all their eggs. This suggests that energetic reserves were exhausted before
488 egg stock, which is surprising given the extremely short freshwater migration required to reach
489 spawning grounds in the Nivelle.

490 Combining acceleration and temperature data collected in the field to equations parametrized
491 in laboratory experiments, we attempted to estimate the energetic expenditure of spawning shad.
492 Total energy expenditure ranged from 4856 to 9743 kJ (mean=7193). This is quite high, compared to
493 female American shad, which entered the Connecticut river with a stock of 12 000 kJ, of which
494 approximately 5 000 kJ were consumed along their 228-km and seven-week long upstream migration
495 (Leonard & McCormick, 1999). According to calculated energy expenditure, the energetic model
496 predicted that shad should have lost on average 13% of their initial weight, which was much less than
497 the observed 42% loss. Of course, the energetic model did not account for egg expulsion, which must
498 represent a large proportion of weight loss, given that ovaries can represent up to 15% of somatic
499 weight at the onset of the spawning season (Cassou-Leins & Cassou-Leins, 1981; Taverny, 1991).
500 Moreover, the equations used to convert TBF and temperature to energy expenditure and weight loss
501 were not parametrized with data obtained on *A. alosa* but on *A. sapidissima* (Castro-Santos & Letcher,
502 2010; Leonard et al., 1999; Leonard & McCormick, 1999) which is the species most closely related to
503 *A. alosa* for which such reliable information exist. Although American shad and Allis shad have the

504 same morphology and ecology, some elements suggest that results on American shad could not exactly
505 apply to our study on Allis shad. First, although the range of temperature used by Leonard et al. (1999)
506 to link swim speed and temperature to energy expenditure were the same as the temperature
507 encountered by shad in our study, TBF of Allis shad in the field exceeded the fastest swim tested by
508 Leonard et al. (1999). In particular, the brief bouts of very high TBF which correspond to spawning acts
509 may represent anaerobic efforts, which are more costly than aerobic effort observed by Leonard et al.
510 (1999). By the way, the volleys of spawning acts performed by females in a few tens of minutes could
511 lead to sexual selection of traits affecting the recovery after sprint (Kieffer, 2000). Second, the
512 relationship linking swim speed to oxygen demand (MO_2), varies between species, even closely related,
513 and American shad seems to have a particularly high metabolism compared to other clupeids (Leonard
514 et al., 1999). This would have led to an overestimation of energy expense for *A. alosa*. Third, the
515 relative contribution of lipids and proteins as metabolic fuel may differ between the iteroparous
516 American shad and the semelparous Allis shad. Indeed, as migratory iteroparous fishes have to spare
517 proteins, especially in the red muscle, for their downstream migration, semelparous species can
518 exhaust their protein stock to complete spawning (Schultz, 1999). Also, Leonard & McCormick (1999)
519 measured the relative expenditure of lipids and proteins in *migrating* American shad, while we
520 monitored *spawning* Allis shad. It has been shown that most anadromous fishes catabolise proteins
521 only when lipid reserves have been exhausted, in a way that lipids mainly fuel migration while proteins
522 fuel spawning (Beamish, Potter, & Thomas, 1979; Hendry & Berg, 1999; Idler & Bitners, 1958; Jonsson,
523 Jonsson, & Hansen, 1997). Given that proteins have a lower energy density than lipids, the surprising
524 high energy consumption and the low weight loss predicted by the energetic model may be explained
525 by spawning Allis shad relying more on proteins than on lipids. However, Allis shad in our study, like
526 Atlantic salmon in Hendry & Beall (2004), had only migrated 13 km in freshwater before the onset of
527 spawning and monitoring, so their lipid stores were probably still high. Although we did not
528 characterize body composition, the average initial Fulton's coefficient of condition in our study was
529 1.2, against 1.56 at the 250th km in the Garonne and 0.96 at the 80th km in the Douro, both in May

530 (Cassou-Leins & Cassou-Leins, 1981). In such longer rivers, the management of energy and egg stock is
531 certainly more challenging (Castro-Santos & Letcher, 2010), especially if dams impose additional
532 swimming costs, warm water (due to global change, river fragmentation and water withdrawal)
533 increases metabolism, and global change disturbs food availability at sea.

534 Beside the estimation of energetic costs from dynamic acceleration, the continuous estimation
535 of body roundness from static acceleration is a promising yet perfectible application. Gravitational
536 acceleration is commonly used to infer the posture of the animal, assuming that the position of the
537 accelerometer on the animal is constant. Here, assuming that shad stayed upright for most of the time,
538 gravitational acceleration was used as an indicator of change in body shape. In particular, we
539 hypothesized that the angle θ between the *x* axis of the accelerometer and the vertical may indicate
540 body roundness. As expected, θ was positively correlated to Fulton coefficient of condition, and
541 decreased along the spawning season, as fish thinned. The accelerometer was attached under the
542 dorsal fin, where the cross-section is the broadest, which probably maximized the sensitivity of
543 acceleration data to fish thinning. Furthermore, shad mainly store energy for migration and spawning
544 as subdermal fat and interstitial fat in the white muscle (Leonard & McCormick, 1999), and the limited
545 consumption of visceral and liver fat, may not have affected θ. However, the shift in θ was not
546 correlated to weight loss during the spawning season. This could be due to interindividual differences
547 in the exact position of the accelerometers on the fish, or in the relationship between weight and
548 roundness. Indeed, weight loss due to gamete expulsion was probably undetectable by the
549 accelerometer attached to the back of the fish, as suggested by the absence of effect of spawning acts
550 on the variation of θ during a night. Given that ovaries can represent up to 15% of a shad weight at
551 arrival on spawning grounds (Cassou-Leins & Cassou-Leins, 1981; Taverny, 1991), a significant loss of
552 weight was probably not reflected in the rotation of the accelerometer across the spawning season. In
553 fact, shift of θ across eight hour periods increased with neither TBF nor temperature, contrary to what
554 was expected from the relationship linking TBF and temperature to energy consumption in American
555 shad (Leonard et al., 1999). According to the linear mixed model, the angle θ only shifted more during

nights than during mornings or afternoons, and TBF was higher during nights, but the effect of TBF itself was not significant. Additionally, θ sometimes increased from one period to the next, and fluctuated a lot especially at the end of the season, so it was clearly affected by other processes than fish thinning. In particular, while the attachment wires were tighten during the tagging procedure, fish thinning loosened them so the accelerometer must have jiggled more and more as fish thinned. Hence, using the angle of the accelerometer to quantitatively track change in weight or body roundness will certainly require further tuning, such as laboratory experiment with repeated weighing and image analysis of cross-section, or drastic standardization of attachment procedure, but we consider it a promising method to monitor individual condition in the field. Beyond thinning due to energy consumption, this approach could be used to detect the many ecologically or behaviourally relevant changes in animal shape, such as parturition, massive food intake in large predators, swelling due to tissue inflammation, or inflation as a courtship or defence behaviour (Brainerd, 1994; Bruning, Phillips, & Shine, 2010). Combined with dynamic acceleration, such data could be used to test whether these changes in shape are associated to global activity or to the expression of specific behaviours.

Acknowledgements

The authors thank the experimental facility ECP for its help in capturing and tagging the fish, and B. Liquet, F. Luthon, B. Larroque and E. Bouix for their help in the initial exploration of data. All experimental procedures comply with French and European legislation, and were approved by the legal representative (prefectural decree #64-2017-04-25-004) and the ethical committee for birds and fishes in the French region Nouvelle Aquitaine (authorization #2016020116037869). This study was financed by the French Agency for Biodiversity, the Adour-Garonne Water Agency, and the French region Nouvelle Aquitaine.

References

Acolas, M. L., Anras, M. L. B., Véron, V., Jourdan, H., Sabatié, M. R., & Baglinière, J. L. (2004). An assessment of the upstream migration and reproductive behaviour of allis shad (*Alosa alosa* L.) using acoustic tracking. *ICES Journal of Marine Science: Journal Du Conseil*, *61*(8), 1291–1304. doi:10.1016/j.icesjms.2004.07.023

Acolas, M., Veron, V., Jourdan, H., Begout, M., Sabatie, M., & Bagliniere, J. l. (2006). Upstream migration and reproductive patterns of a population of allis shad in a small river (L'Aulne, Brittany, France). doi:DOI:10.1016/j.icesjms.2005.05.022

Anderson, S. S., & Fedak, M. A. (1985). Grey seal males: energetic and behavioural links between size and sexual success. *Animal Behaviour*, *33*(3), 829–838. doi:10.1016/S0003-3472(85)80017-8

Baglinière, J.-L., & Elie, P. (2000). *Les Aloses (Alosa alosa et Alosa fallax spp.): écobiologie et variabilité des populations*. Editions Quae.

Bates, D., Maechler, M., Bolker, B., & Walker, S. (2014). lme4: Linear mixed-effects models using Eigen and S4 (Version R package version 1.1-7).

Beamish, F. W. H., Potter, I. C., & Thomas, E. (1979). Proximate composition of the adult anadromous sea lamprey, *Petromyzon marinus*, in relation to feeding, migration and reproduction. *Journal of Animal Ecology*, *48*(1), 1–19. doi:10.2307/4096

Bengen, G. S. H. (1992). *Suivi de la maturation gonadique des aloses, Alosa alosa L. lors de leur migration en Garonne* (Thèse de doctorat). Institut national polytechnique, Toulouse, France.

Bonnet, X., Bradshaw, D., & Shine, R. (1998). Capital versus income breeding: an ectothermic perspective. *Oikos*, *83*(2), 333–342.

Borgia, G. (1985). Bower quality, number of decorations and mating success of male satin bowerbirds (*Ptilonorhynchus violaceus*): an experimental analysis. *Animal Behaviour*, *33*(1), 266–271. doi:10.1016/S0003-3472(85)80140-8

Brainerd, E. L. (1994). Pufferfish inflation: Functional morphology of postcranial structures in *Diodon holocanthus* (Tetraodontiformes). *Journal of Morphology*, *220*(3), 243–261. doi:10.1002/jmor.1052200304

Breine, J., Pauwels, I. S., Verhelst, P., Vandamme, L., Baeyens, R., Reubens, J., & Coeck, J. (2017). Successful external acoustic tagging of twaite shad *Alosa fallax* (Lacépède 1803). *Fisheries Research*, *191*(Supplement C), 36–40. doi:10.1016/j.fishres.2017.03.003

Brett, J. R., & Groves, T. D. D. (1979). Physiological energetics. In W. S. Hoar, D. J. Randall, & J. R. Brett (Eds.), *Bioenergetics and growth* (Academic Press, Vol. 8, pp. 279–352). New York.

Brooks, M. E., Kristensen, K., Benthem, K. J. van, Magnusson, A., Berg, C. W., Nielsen, A., … Bolker, B. M. (2017). glmmTMB balances speed and flexibility among packages for zero-inflated generalized linear mixed modeling. *The R Journal*, *9*(2), 378–400.

Brown, D. D., Kays, R., Wikelski, M., Wilson, R., & Klimley, A. P. (2013). Observing the unwatchable through acceleration logging of animal behavior. *Animal Biotelemetry*, *1*(1), 1–16. doi:10.1186/2050-3385-1-20

Bruning, B., Phillips, B. L., & Shine, R. (2010). Turgid female toads give males the slip: a new mechanism of female mate choice in the Anura. *Biology Letters*, *6*(3), 322–324. doi:10.1098/rsbl.2009.0938

Casas, J., Pincebourde, S., Mandon, N., Vannier, F., Poujol, R., & Giron, D. (2005). Lifetime nutrient dynamics reveal simultaneous capital and income breeding in a parasitiod. *Ecology*, *86*(3), 545–554. doi:10.1890/04-0812

Cassou-Leins, F., & Cassou-Leins, J.-J. (1981). *Recherches sur la biologie et l'halieutique des migrateurs de la Garonne et principalement l'alose : Alosa alosa* (Thèse de doctorat). Institut National Polytechnique de Toulouse.

Castro-Santos, T., & Letcher, B. H. (2010). Modeling migratory energetics of Connecticut River American shad (*Alosa sapidissima*): implications for the conservation of an iteroparous anadromous fish. *Canadian Journal of Fisheries and Aquatic Sciences*, *67*(5), 806–830. doi:10.1139/F10-026

Chanseau, M., Castelnaud, G., Carry, L., Martin-Vandembulcke, D., & Belaud, A. (2004). Essai d'évaluation du stock de géniteurs d'alose *Alosa alosa* du bassin versant Gironde-Garonne-Dordogne sur la période 1987-2001 et comparaison de différents indicateurs d'abondance. *Bulletin Français de La Pêche et de La Pisciculture*, (374), 1–19. doi:10.1051/kmae:2004023

Collins, P. M., Halsey, L. G., Arnould, J. P. Y., Shaw, P. J. A., Dodd, S., & Green, J. A. (2016). Energetic consequences of time-activity budgets for a breeding seabird. *Journal of Zoology*, *300*(3), 153–162. doi:10.1111/jzo.12370

Craig, J. F., Kenley, M. J., & Talling, J. F. (1978). Comparative estimations of the energy content of fish tissue from bomb calorimetry, wet oxidation and proximate analysis. *Freshwater Biology*, *8*(6), 585–590. doi:10.1111/j.1365-2427.1978.tb01480.x

Emlen, S. T., & Oring, L. W. (1977). Ecology, sexual selection, and the evolution of mating systems. *Science*, *197*(4300), 215–223. doi:10.1126/science.327542

Fatin, D., & Dartiguelongue, J. (1996). *Etude préliminaire de la reproduction des aloses en 1995 entre Tuilières et Mauzac sur la Dordogne* (Rapport S.C.E.A.) (p. 39pp).

Gauthey, Z., Freychet, M., Manicki, A., Herman, A., Lepais, O., Panserat, S., … Labonne, J. (2015). The concentration of plasma metabolites varies throughout reproduction and affects offspring number in wild brown trout (*Salmo trutta*). *Comparative Biochemistry and Physiology Part A: Molecular & Integrative Physiology*, *184*, 90–96. doi:10.1016/j.cbpa.2015.01.025

Goldstein, D. L. (1988). Estimates of daily energy expenditure in birds: The time-energy budget as an integrator of laboratory and field studies. *American Zoologist*, *28*(3), 829–844.

Groscolas, R., Viera, V., Guerin, N., Handrich, Y., & Côté, S. D. (2010). Heart rate as a predictor of energy expenditure in undisturbed fasting and incubating penguins. *Journal of Experimental Biology*, *213*(1), 153–160. doi:10.1242/jeb.033720

Handrich, Y., Bevan, R. M., Charrassin, J.-B., Butler, P. J., Ptz, K., Woakes, A. J., … Maho, Y. L. (1997). Hypothermia in foraging king penguins. *Nature*, *388*(6637), 64–67. doi:10.1038/40392

Heimpel, G. E., & Rosenheim, J. A. (1998). Egg Limitation in Parasitoids: A Review of the Evidence and a Case Study. *Biological Control*, *11*(2), 160–168. doi:10.1006/bcon.1997.0587

Hendry, A. P., & Beall, E. (2004). Energy use in spawning Atlantic salmon. *Ecology of Freshwater Fish*, *13*(3), 185–196. doi:10.1111/j.1600-0633.2004.00045.x

Hendry, A. P., & Berg, O. K. (1999). Secondary sexual characters, energy use, senescence, and the cost of reproduction in sockeye salmon. *Canadian Journal of Zoology*, *77*(11), 1663–1675. doi:10.1139/z99-158

Hicks, O., Burthe, S., Daunt, F., Butler, A., Bishop, C., & Green, J. A. (2017). Validating accelerometry estimates of energy expenditure across behaviours using heart rate data in a free-living seabird. *Journal of Experimental Biology*, jeb.152710. doi:10.1242/jeb.152710

Hughes, P. W. (2017). Between semelparity and iteroparity: Empirical evidence for a continuum of modes of parity. *Ecology and Evolution*, *7*(20), 8232–8261. doi:10.1002/ece3.3341

Idler, D. R., & Bitners, I. (1958). Biochemical studies on sockeye salmon during spawning migration: Ii. Cholesterol, fat, protein, and water in the flesh of standard fish. *Canadian Journal of Biochemistry and Physiology*, *36*(8), 793–798. doi:10.1139/o58-084

Jepsen, N., Thorstad, E. B., Havn, T., & Lucas, M. C. (2015). The use of external electronic tags on fish: an evaluation of tag retention and tagging effects. *Animal Biotelemetry*, *3*(1), 49. doi:10.1186/s40317-015-0086-z

Jonsson, N., Jonsson, B., & Hansen, L. P. (1997). Changes in proximate composition and estimates of energetic costs during upstream migration and spawning in Atlantic salmon *Salmo salar*. *Journal of Animal Ecology*, *66*(3), 425–436. doi:10.2307/5987

Kieffer, J. D. (2000). Limits to exhaustive exercise in fish. *Comparative Biochemistry and Physiology. Part A, Molecular & Integrative Physiology*, *126*(2), 161–179.

Langkau, M. C., Clavé, D., Schmidt, M. B., & Borcherding, J. (2016). Spawning behaviour of Allis shad *Alosa alosa*: new insights based on imaging sonar data. *Journal of Fish Biology*, *88*(6), 2263–2274. doi:10.1111/jfb.12978

Leonard, J. B. K., Norieka, J. F., Kynard, B., & McCormick, S. D. (1999). Metabolic rates in an anadromous clupeid, the American shad (*Alosa sapidissima*). *Journal of Comparative Physiology B*, *169*(4–5), 287–295. doi:10.1007/s003600050223

Leonard, J. B. K., & McCormick, S. D. (1999). Effects of migration distance on whole-body and tissue-specific energy use in American shad (*Alosa sapidissima*). *Canadian Journal of Fisheries and Aquatic Sciences*, *56*(7), 1159–1171. doi:10.1139/f99-041

Mennesson-Boisneau, C., & Boisneau, P. (1990). *Migration, répartition, reproduction, caractéristiques biologiques et taxonomie des aloses (Alosa sp) dans le bassin de la loire* (Thèse de doctorat). Université de Rennes et Paris XII.

Nagy, K. A., Girard, I. A., & Brown, T. K. (1999). Energetics of free-ranging mammals, reptiles, and birds. *Annual Review of Nutrition*, *19*, 247–277. doi:10.1146/annurev.nutr.19.1.247

Petersson, E., & Jarvi, T. (2001). “False orgasm” in female brown trout: trick or treat? *Animal Behaviour*, *61*(2), 497–501. doi:10.1006/anbe.2000.1585

Pianka, E. R. (1976). Natural selection of optimal reproductive tactics. *American Zoologist*, *16*(4), 775–784.

R Development Core Team. (2008). *R: A language and environment for statistical computing.* R Foundation for Statistical Computing, Vienna, Austria. Retrieved from http://www.R-project.org

Rands, S. A., Houston, A. I., & Cuthill, I. C. (2006). Measurement of mass change in breeding birds: A bibliography and discussion of measurement techniques. *Ringing & Migration*, *23*(1), 1–5. doi:10.1080/03078698.2006.9674337

Roff, D. (1993). *Evolution Of Life Histories: Theory and Analysis*. Springer Science & Business Media.

Rougier, T., Lambert, P., Drouineau, H., Girardin, M., Castelnaud, G., Carry, L., … Rochard, E. (2012). Collapse of allis shad, *Alosa alosa*, in the Gironde system (southwest France): environmental change, fishing mortality, or Allee effect? *ICES Journal of Marine Science: Journal Du Conseil*, *69*(10), 1802–1811. doi:10.1093/icesjms/fss149

Schultz, D. L. (1999). Comparison of lipid levels during spawning in annual and perennial darters of the subgenus Boleosoma, *Etheostoma perlongum*, and *Etheostoma olmstedi*. *Copeia*, *1999*(4), 906–916. doi:10.2307/1447966

Stearns, S. C. (1992). *The Evolution of Life Histories*. OUP Oxford.

Steinbach, P., Gueneau, P., Autuoro, A., & Broussard, D. (1986). Radio-pistage de grandes aloses adultes en Loire. *Bulletin Français de La Pêche et de La Pisciculture*, (302), 106–117. doi:10.1051/kmae:1986007

Taverny, C. (1991). *Contribution à la connaissance de la dynamique des populations d'aloses : Alosa Alosa et Alosa Fallax dans le système fluvio-estuarien de la Gironde : pêche, biologie et écologie : étude particulière de la devalaison et de l'impact des activités humaines*. Bordeaux 1. Retrieved from http://www.theses.fr/1991BOR10535

Tétard, S., Feunteun, E., Bultel, E., Gadais, R., Bégout, M.-L., Trancart, T., & Lasne, E. (2016). Poor oxic conditions in a large estuary reduce connectivity from marine to freshwater habitats of a diadromous fish. *Estuarine, Coastal and Shelf Science*, *169*, 216–226. doi:10.1016/j.ecss.2015.12.010

Wilson, R. P., White, C. R., Quintana, F., Halsey, L. G., Liebsch, N., Martin, G. R., & Butler, P. J. (2006). Moving towards acceleration for estimates of activity-specific metabolic rate in free-living animals: the case of the cormorant. *The Journal of Animal Ecology*, *75*(5), 1081–1090. doi:10.1111/j.1365-2656.2006.01127.x

Wright, S., Metcalfe, J. D., Hetherington, S., & Wilson, R. (2014). Estimating activity-specific energy expenditure in a teleost fish, using accelerometer loggers. *Marine Ecology Progress Series*, *496*, 19–32. doi:10.3354/meps10528

Yamazaki, C., & Koizumi, I. (2017). High frequency of mating without egg release in highly promiscuous nonparasitic lamprey *Lethenteron kessleri*. *Journal of Ethology*, *35*(2), 237–243. doi:10.1007/s10164-017-0505-0